Food Chemistry 406 (2023) 135039

Contents lists available at ScienceDirect

Food Chemistry

journal homepage: www.elsevier.com/locate/foodchem

Silk fibroin-based colorimetric microneedle patch for rapid detection of spoilage in packaged salmon samples

Jiang-Yue Wang [a,b,c], Li-Jian Chen [a,b,c,*], Xu Zhao [a,b,c], Xiu-Ping Yan [a,b,c,d,*]

[a] State Key Laboratory of Food Science and Technology, Jiangnan University, Wuxi 214122, China
[b] International Joint Laboratory on Food Safety, Jiangnan University, Wuxi 214122, China
[c] Institute of Analytical Food Safety, School of Food Science and Technology, Jiangnan University, Wuxi 214122, China
[d] Key Laboratory of Synthetic and Biological Colloids, Ministry of Education, School of Chemical and Material Engineering, Jiangnan University, Wuxi 214122, China

ARTICLE INFO

Keywords:
Silk fibroin
Microneedle patch
Colorimetric sensor
Nondestructive detection
Packaged salmon spoilage

ABSTRACT

Spoiled salmon can cause foodborne diseases and severely affects human health. Herein, we report a pH-responsive colorimetric microneedle (MN) patch fabricated from bromothymol blue (BTB) and silk fibroin meth acryloyl (SilMA) (BTB/SilMA@MN patch) for sensing salmon spoilage. The needle tips of MN could penetrate food cling film and insert into fish to extract tissue fluids directly and transport the extracted fluids to the backing layer for color displaying. The color change of BTB/SilMA@MN patches depended on the pH variation resulting from the increase of total volatile basic nitrogen in salmon during storage. The color of MN patches changed from yellow to yellowish green and to final green, indicating salmon changed from fresh to medium fresh and then to putrefied, respectively. Salmon spoilage can be rapidly determined via naked eye recognition and also analyzed on a smartphone in a nondestructive way, allowing consumers to estimate food quality easily and reliably.

1. Introduction

Eating spoiled seafood especially raw fish and mollusks can cause illnesses ranging from mild gastroenteritis to life-threatening diseases (Amagliani, Brandi, & Schiavano, 2012). Salmon is recognized as a healthy food due to its richness of high-quality proteins, omega-3 fatty acids, fundamental micronutrients and minerals (Amagliani, Brandi, & Schiavano, 2012). Consumer consumption of salmon has increased sharply in recent years. As sashimi and sushi are the main market circulation forms for salmon (Fan et al., 2021), freshness is one of the most important factors to determine the quality of raw fish. However, salmon is a highly corruptible food, and the quality is influenced by numerous factors such as the packaging material, treatment process, and preservation condition (Feng, Zhang, Liu, Liu, & Zhang, 2020; Zhu, Gao, Gao, & Sun, 2018). Therefore, it is crucial for rapid and effective detection of the freshness of packaged salmon.

Detection of fish and meat freshness mainly includes organoleptic evaluation, microbial detection and spectroscopic methods, such as near-infrared reflectance spectroscopy, hyperspectral imaging, and fluorescence spectroscopy (Cheng and Sun, 2015; Prabhakar, Vatsa, Srivastav, & Pathak, 2020). Traditional organoleptic evaluation perceives product sensory characteristics, containing appearance, color, smell, texture and taste through subjective judgments of evaluators (Wu, Zhang, Chen, & Bhandari, 2021). Sensory evaluators and consumers may have different responses to the same stimulus level, leading to inaccurate test results originating from the non-objective judgments (Liu et al., 2019). Moreover, microbial detection and spectroscopic methods are limited for applications because of their tedious operation and relatively high cost. Therefore, rapid and cost-effective detection techniques to monitor the freshness and quality of fish/meat have emerged increasingly (Wu, Zhang, Chen, & Bhandari, 2021).

Colorimetric sensors on the packaging film have attracted great attention because of their nondestructive way to monitor the freshness of fish/meat without the need for sample pretreatment (Li, Lin, Wang, Lv, & Li, 2019; Chang, Li, Hou, Duan, & Li, 2018; Li, Lin, Lv, Gai, & Li, 2020). Microbes contaminated fish/meat always releases total volatile basic nitrogen (TVB-N), such as ammonia and amines produced from protein decay, leading to pH increase in fish and meat and their packaging environment (Ezati, Priyadarshi, Bang, & Rhim, 2021; Alamdari, Forghani, Salmasi, Almasi, Moradi, & Molaei, 2022). Colorimetric sensors designed on the packaging film known as intelligent packaging for the visualization of pH change are popular for rapid detection of fish/

* Corresponding authors at: Institute of Analytical Food Safety, School of Food Science and Technology, Jiangnan University, Wuxi 214122, China.
E-mail addresses: chenlijian123@jiangnan.edu.cn (L.-J. Chen), xpyan@jiangnan.edu.cn (X.-P. Yan).

https://doi.org/10.1016/j.foodchem.2022.135039
Received 14 August 2022; Received in revised form 28 October 2022; Accepted 20 November 2022
Available online 23 November 2022

meat spoilage (Liu et al., 2019). Chemical chromogenic dyes can rapidly and visually monitor the freshness of packaging food based on pH-responsive activities (Chen, Zhang, Bhandari, & Guo, 2018). Cao et al. prepared an anchored bromothymol blue (BTB) film for the freshness monitoring of chicken and pork (Cao, Sun, Zhang, Liu, Li, & Wang, 2019). BTB as pH-sensitive dye was also incorporated into hydrogel as an indicator for the detection of TVB-N/pH during pork storage at 4 °C based on color change (Sutthasupa, Padungkit, & Suriyong, 2021). Obvious pH responsive color change of BTB demonstrated the good potential of BTB dye-based sensors for real-time indication of meat spoilage. These non-direct-contact colorimetric sensors effectively avoid dye migration and potential second pollution (Liu et al., 2022). However, they can only sense volatile substances in the packaging headspace, and often give delayed information.

Direct-contact sensor provides real-time and accurate information to judge the fish and meat spoilage. Kim et al. developed a bromocresol purple dye-based colorimetric sensor with pH-responsive activity to monitor the freshness of chicken breast meat by direct surface contact (Kim, Lee, Lee, Baek, & Seo, 2017). The bromocresol violet dye was immobilized within high moisture-absorbing materials including polyvinyl alcohol, and exhibited color change from yellow to blue and finally purple to point spoilage of chicken breast meat. Direct-contact colorimetric sensors with high absorption efficiency and good safety are still urgently required.

Microneedle (MN) patches, containing an array of miniaturized needles, have emerged as promising tools for biomedical applications, such as drug delivery, biomarker detection, and health monitoring (Rad, Prewett, & Davies, 2021; Yang et al., 2021; Dixon et al., 2021). Swellable hydrogel-based MN arrays extract biomolecules in blood and interstitial fluid within a few minutes or even seconds. They also can be applied to extract target analytes from food samples (Li, Feng, Wang, Liu, Chen, & Fu, 2021). Silk fibroin is a non-toxic and edible natural polymer with excellent mechanical strength and high hydrophilicity (Kim et al., 2018). Meth acryloyl functionalized silk fibroin meth acryloyl (SilMA) is more apt to be crosslinked than silk fibroin under UV light to improve its stability and mechanical strength for MN patch preparation (Bae, Kim, & Park, 2020). However, no MN patch using SilMA as raw material has been reported for monitoring the change of TVB-N/pH during fish/meat storage.

Herein, we report the exploration of SilMA as the substrate and BTB as the chromogenic agent to fabricate a colorimetric MN patch (BTB/SilMA@MN) for pH-responsive detection of packaged salmon spoilage without unpacking and pre-treatment. The tips of BTB/SilMA@MN patch enable penetrating the packaging film to sample fluid deep in salmon tissue, allowing fluid to flow into the chromogenic dye reservoir of backing layer in patch. pH variation in connection with the freshness of salmon is indicated by the color change of BTB from yellow to yellowish green and to final green. Furthermore, the RGB values in the pictures of chromogenic MN patches are quantitatively analyzed with the Color Coll APP on a smart phone, giving a good linear relationship with TVB-N content. The proposed MN patches can accurately and conveniently indicate fish spoilage in real-time and on-site, showing great potential for food safety application.

2. Materials and methods

2.1. Materials

SilMA and lithium phenyl (2,4,6-trimethylbenzoyl) phosphinate (LAP) came from Engineering for Life Intelligent Equipment (Suzhou, China). Polydimethylsiloxane (PDMS) mold (12 mm × 12 mm in size, 8 × 8 MNs conical cavity array with 1500 μm in height, 550 μm in diameter of the base) was from Taizhou Microchip Medical Technology (Taizhou, China). Horseradish peroxidase (HRP) lyophilized powder was from Shanghai Maclin Biochemical Technology Co. (Shanghai, China). Hydrogen peroxide (H_2O_2, 30 %) was obtained from Sinopharm Chemical Reagent (Shanghai, China). Atlantic salmon (*Salmo salar*) samples were purchased from Shenzhen Feng Xian Food Co. (Shenzhen, China). Ultrapure water was purchased from Wahaha Group Co. (Hangzhou, China). All reagents were of analytical grade and used without further purification.

2.2. Preparation of BTB/SilMA@MN patch

2.2.1. Preparation of SilMA hydrogel solution

LAP (0.05 g) as light initiator was dissolved in ultrapure water (20 mL) and LAP solution (0.25 %, w/v) was obtained after shaking at 45 °C for 30 min. Then, SilMA (0.07 g) was added to LAP solution (1 mL) in polyethylene tube and placed at room temperature for 1 h for complete dissolution to obtain 7 % (w/v) SilMA hydrogel solution.

2.2.2. Fabrication of MN patch tips

SilMA hydrogel solution (250 μL, 7 % w/v) was added to the PDMS mold and the foam was removed under negative pressure (1.0 MPa) with a vacuum drying chamber (DZK-K50B, Darth Carter, China) at 35 °C for 5 min. The excess surface hydrogel solution was also removed. The solution in PDMS mold was concentrated and dried in a thermostatic blast oven (DGT-TG80, Darth Carter, China) at 37 °C for 6 h. The above procedure was repeated for 3 times to fill the tip microcavity with hydrogel. Finally, the hydrogel in the tips was irradiated with a handheld UV lamp (254 nm) for 150 s and the mold was taken out to obtain photocurable MN tips.

2.2.3. Fabrication of backing layer in MN patch

BTB (0.1 g) was fully dissolved in 20 % ethanol solution to obtain BTB solution (0.1 %, w/v). BTB solution (400 μL) and water (330 μL) were added to SilMA (0.07 g) in a polyethylene tube to make SilMA completely dissolve. Then, HRP (135 μL, 150 U/mL) and H_2O_2 (135 μL, 100 mM) were severally added to above solutions to obtain BTB hydrogel solution (0.04 %, w/v). BTB hydrogel solution (200 μL, 0.04 %, w/v) was dripped onto the mold containing the as-prepared MN tips and the mold was dried at 37 °C for 12 h. Then, the mold was peeled to obtain colorimetric hydrogel BTB/SilMA@MN patch.

2.3. Characterization of BTB/SilMA@MN patch

2.3.1. Surface morphology

The morphology of the prepared MN patches was observed on a stereomicroscope (SGO-SZMN45TRB4, KWONG KUK, China).

2.3.2. Mechanical properties

The mechanical properties of MN tips prepared with different SilMA concentrations were analyzed on a texture analyzer (TA-XT PLUS, Stable Micro System, UK). Probe was selected P/25. Parameter setting: The measurement mode and option were gel; the force sensor approached tips at the speed of 1 mm/s; the force measurement started when the sensor touched the tips, the measurement rate was 0.2 mm/s; and the measurement ended when the sensor moved 0.5 mm; triggering force was 5 g.

2.3.3. Water absorption

Gelatin hydrogels (3 %, w/v) were prepared by dissolving gelatin (3.0 g) in ultrapure water (100 mL) at 60 °C. Then, gelatin solution was poured on a petri dish and solidified at room temperature for 12 h (Sun et al., 2021). Finally, the dried MN tips were inserted into the gelatin with an appropriate pressure, and the MNs water absorption changes were recorded every 2 min. The water on tip surface was absorbed using absorbent paper, and weight was recorded after placing on filter paper. The water absorption was calculated using equation (1):

$$\text{Water absorption}\% = [(M - M_0) / M_0] \times 100 \quad (1)$$

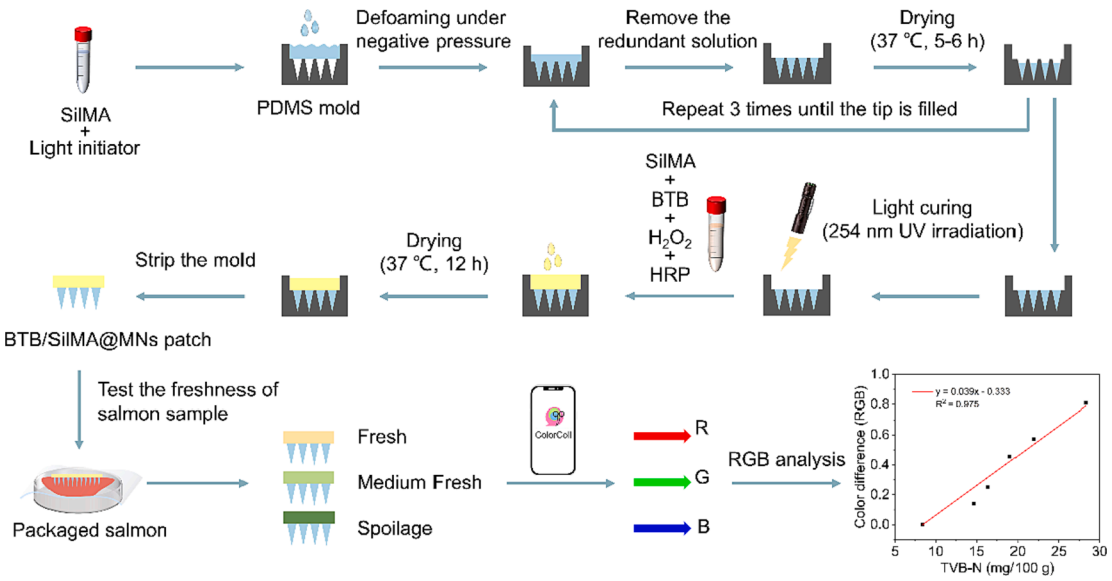

Fig. 1. Schematic illustration for the preparation and application of BTB/SilMA@MN patch for visual monitoring of salmon freshness.

where M_0 was the dry weight of MN tips before the tips inserted into the gelatin, and M was the total weight of MN tips after insertion into the gelatin.

2.3.4. Color pictures

Photos were taken with a mobile phone (iPhone 12 Pro Max, Apple Computer Inc, America). The average RGB pixel intensities were collected on mobile phone application "Color Coll" (IOS operating system) and analyzed with the Adobe Photoshop CC 2019 software. Normalized R′, G′, and B′ values were calculated using the following relationships: $Rx' = Rx/R_{wb}$, $Gx' = Gx/G_{wb}$, and $Bx' = Bx/B_{wb}$, respectively, where "x" represented the data obtained at a certain time and "wb" represented the data obtained in white background (Park, Baynes, Cho, & Yoon, 2014), "0" represented the data obtained from hydrogel without adding buffer solution. Then, the color difference of the hydrogel was calculated as the formula (2) (Lee, Baek, Kim, & Seo, 2019) and the linear relationship was compared:

$$\text{Color difference (RGB)} = [(R_X' - R_0')^2 + (G_X' - G_0')^2 + (B_X' - B_0')^2]^{1/2} \quad (2)$$

2.4. Detection of salmon spoilage with BTB/SilMA@MN patch

Salmon samples (back tissue and muscle, 5 g) were placed in glass petri dishes and sealed with food plastic wrap. Samples were stored at 0 °C and 4 °C for 10 days. The tips of BTB/SilMA@MN patches pierced into plastic wrap and inserted on the salmon tissues. The color changes were recorded as smartphone photography every day without taking down the patches. After storing at 0 °C and 4 °C for 10 days, new BTB/SilMA@MN patches were pasted on the salmon samples across the plastic films. Pictures were taken on the smartphone every 2 min.

The pH values of salmon samples were recorded on a digital pH meter (ST3100, OHAUS, USA). Samples (2 g) were firstly blended with ultrapure water (20 mL) using a high-speed dispersing machine (T18 digital ULTRA-TURRAX, IKA, Germany) to homogenize for 3 min. All tests were performed in triplicate.

The TVB-N levels of salmon samples were tested according to the method of Ding et al. (Ding, Li, & Li, 2014). The homogenized salmon samples (5 g) were crushed with a meat grinder. Then, MgO (0.5 g) powder was added into the digestive tube and fully mixed with the salmon samples. Finally, the digestive tube containing the prepared salmon samples was connected to automatic Kjeldahl nitrogen analyzer (K9840, Hanon, China) for automatic analysis. The distillate was collected in a conical flask containing boric acid solution (30 mL, 20 g/L), the mixed indicator (12 drops) consisting of methyl red ethanol solution (2 drops, 1 g/L) and bromocresol green ethanol solution (10 drops, 1 g/L). The TVB-N value of the boric acid solution was titrated with hydrochloric acid solution (0.01 M). The analysis was repeated three times to calculate the TVB-N level, expressed as mg/100 g.

The total viable count (TVC) of salmon samples were tested according to Zhu et al. (Zhu, Gao, Gao, & Sun, 2018). In brief, a piece of sample (1 g) was homogenized in 9 mL phosphate buffer saline solution (PBS) (pH 7.2) for 2 min. The homogenized sample solution was diluted ten times with PBS and dispersed on Luria Bertani Broth Agar plates. Then, the plates were incubated at 37 °C for 72 h. The colonies were counted and expressed as lg CFU/g. The tests were performed in triplicate.

2.5. Data analysis

Measurement of each property for samples was performed in triplicate with individually prepared samples as the replicated experimental unit, and the results were presented as mean standard deviation (SD). Curve Fitting was carried out by existing mathematical models embedded in the Origin 2021 software (Origin Lab Co., Northampton, MA, USA).

3. Results and discussion

3.1. Preparation and characterization of BTB/SilMA@MN patch

Fig. 1 illustrates the preparation of BTB/SilMA@MN patch. PDMS mold (12 mm × 12 mm in size, 8 × 8 MNs conical cavity array with 1500 μm in height, 550 μm in diameter of the base) was used for MN patch preparation not only to enable the tips of MN patch to penetrate the plastic wrap and extract enough interstitial fluid from the fish tissue but also to make the MN patch portable and low cost with short preparation time. To achieve rigid and safe MNs for penetrating through the food cling film, SilMA was used as the substrate due to its naturally non-toxic property and enough mechanical strength after curing. The MN tips were solidified under 254 nm UV irradiation. The MN backing layer was cured using crosslinking agents (HRP and H_2O_2) to avoid the destruction of UV light on BTB. The as-prepared MN patches were translucent yellow and took regularly arranged MN array (Fig. 2a-c).

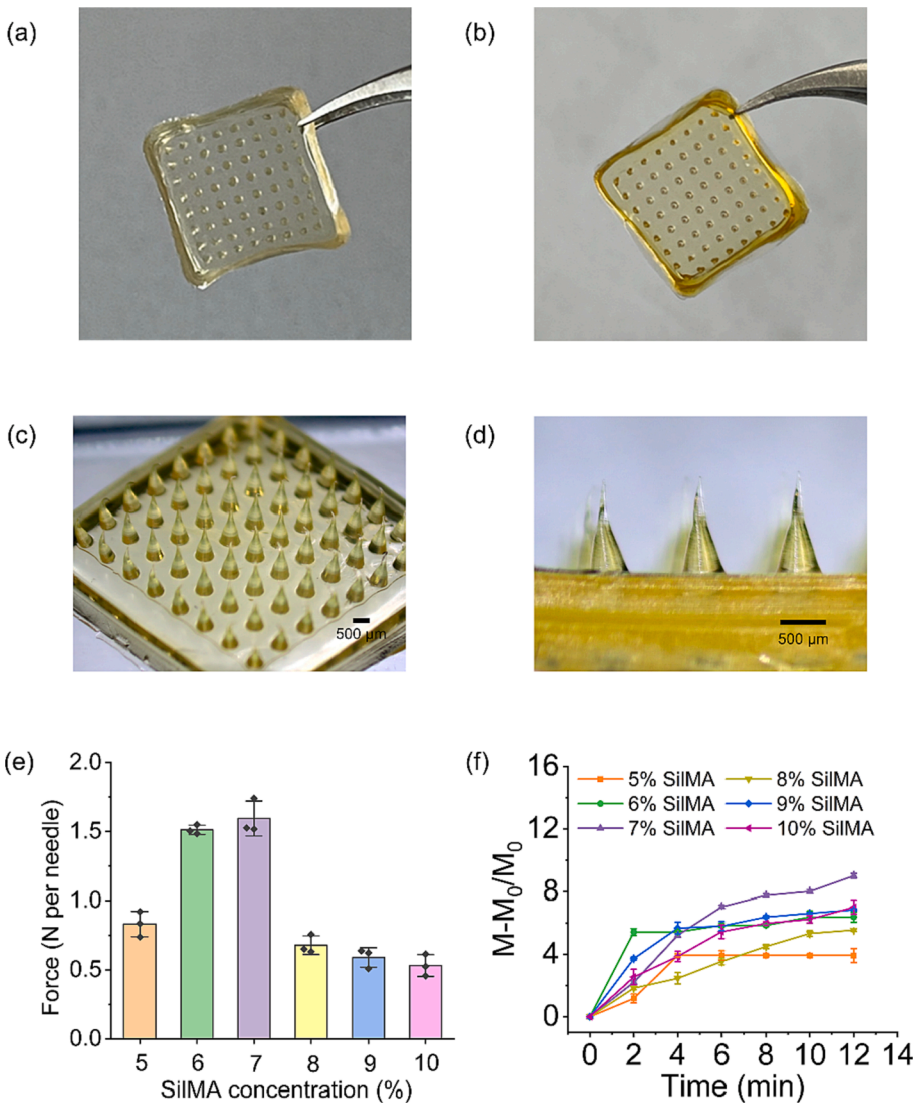

Fig. 2. (a) Photograph of dye-free MN patch; (b) Photograph of the as-prepared BTB/SilMA@MN patch; (c) Microscopy image of BTB/SilMA@MN patch; (d) Local magnified microscopy image of three needle tips in BTB/SilMA@MN patch; (e) Mechanical properties of MN tips with 5%-10% SilMA; (f) Water absorption of MN tips with 5%-10% SilMA.

The yellow color of BTB/SilMA@MN patch was a bit deeper than the MN patch without BTB dye (Fig. 2a, b). The MN array consisted of 8 × 8 conical needles (Fig. 2c). The needle tips showed an average size of 1140.6 ± 15.6 μm in height and 520.3 ± 3.5 μm in diameter (Fig. 2d).

3.2. Mechanical properties of BTB/SilMA@MN patch

To penetrate wrapping packaging with a sufficient mechanical strength, MN patches with different SilMA concentrations (5–10 %, w/v) were prepared and tested. The force–displacement curve of MN patch is shown in Fig. S1. The force was recorded until the displacement of the moving sensor descended by 0.5 mm. The mechanical strength increased with the SilMA concentration up to 7 % w/v, then decreased with a further increase (8–10 %) of the SilMA content (Fig. 2e). The tolerable force of each needle in all patches was above 0.50 N. The needle tips of MN patch with 7 % SilMA could bear the highest force of 1.59 N because the SilMA fully filled the gap in the hydrogel, making the MNs most compact (Yan et al., 2021). The needle tips prepared under this condition were strong enough to penetrate food cling film without breaking (Fig. S2a, S2b). However, when SilMA concentration exceeded to 8 %, MN patches exhibited fracture or plastic failure, and the tolerable forces of needles dropped down. With the increase of SilMA concentration, β-sheet structure of silk fibroin hydrogel increased, inducing the increase of the MN brittleness (Barroso, Man, Villapun, Cox, & Ghag, 2021; Zhao, Zhu, Guan, & Wu, 2021). The result exhibited that BTB/SilMA@MN patch prepared with 7 % SilMA concentration could perform best performance on the mechanical strength.

3.3. Water absorption of BTB/SilMA@MN patch

To present wonderful color response performance, water absorption as an important feature of MN patches with different SilMA concentrations was further tested. With the increase of SilMA concentrations from 5 % to 10 %, the water absorption capacity of BTB/SilMA@MN patches first increased and then decreased, which was consistent with the results of Cheng et al. (Cheng, Tao, Qi, Yin, Kundu, & Lu, 2021) (Fig. 2f). Water absorption ability reached the highest when the SilMA concentration was 7 % for the same reason for mechanical strength. Moreover, water absorption of the MN patch was almost completed within 6 min, and tended to be gentle after 8 min. Thus, the MN patch with 7 % SilMA concentration could extract fluid quickly in 6–8 min for sampling.

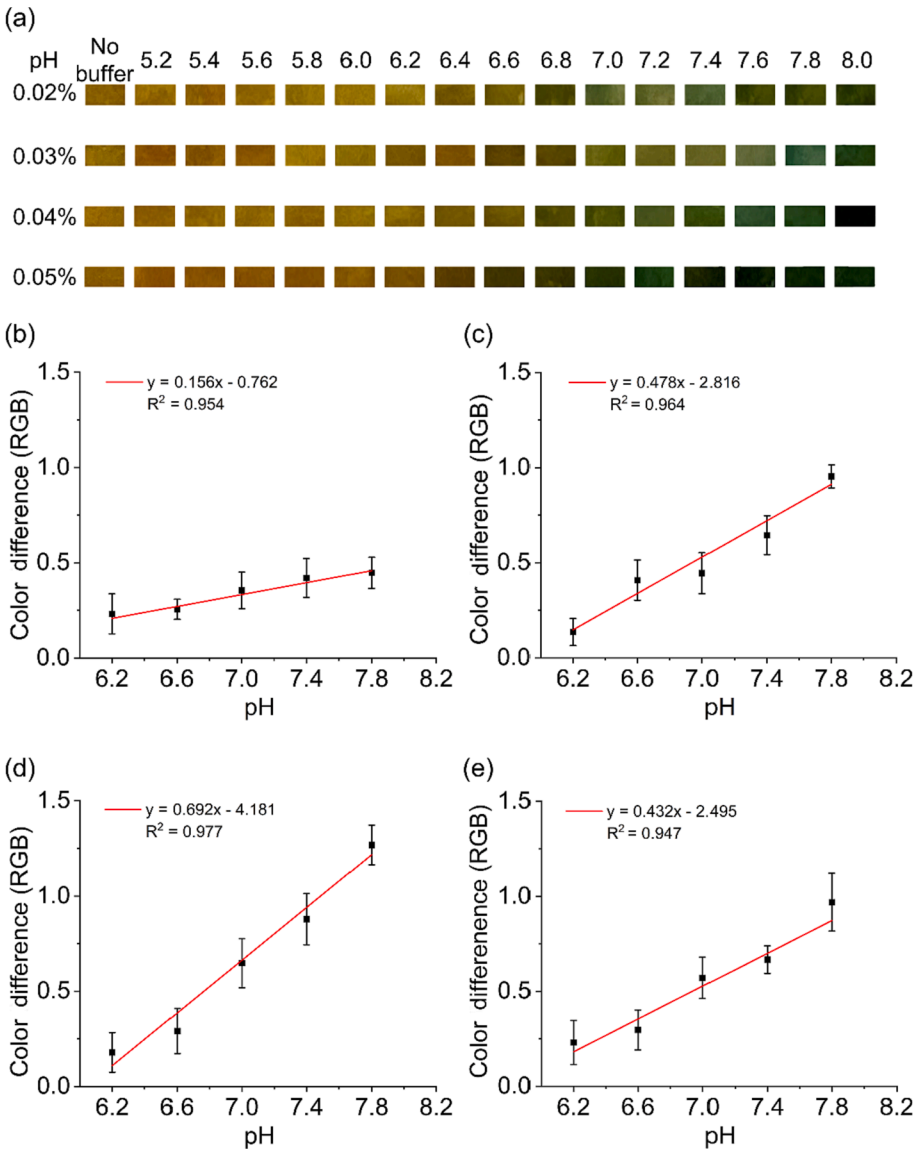

Fig. 3. (a) Color change of BTB-loaded hydrogel with pH. Linear relationships between RGB signals of hydrogel pictures and pH values ranging from 6.2 to 7.8: (b) SilMA hydrogel with 0.02% BTB; (c) SilMA hydrogel with 0.03% BTB; (d) SilMA hydrogel with 0.04% BTB; (e) SilMA hydrogel with 0.05% BTB.

3.4. Optimization of BTB concentration for backing layer

The color of BTB solution changed from yellow to green and final blue with pH from 5.4 to 7.8 (Fig. S3a). Different UV–vis absorption spectra of the BTB solutions with two absorption peaks were observed at various pH values (Fig. S3b). The pH-sensitive intensity and position of the two absorption peaks of the BTB solution changed with pH, indicating that BTB is an ideal indicator for making colorimetric MN patches.

To optimize the BTB concentration in backing layer for preparing BTB/SilMA@MN patch, SilMA hydrogels with different BTB concentrations (0.02 %-0.05 %, w/v) were prepared and exposed to buffer solutions at various pH values (5.2–8.0). The color change of BTB-loaded hydrogel from yellow to green was clearly visible in different pH buffers (Fig. 3a). The BTB-loaded hydrogel showed bright yellow at pH 5.2–6.2, light green at pH 6.4–7.4, and dark green at pH 7.6–8.0. The color difference of the hydrogel depended on BTB concentration. Linear relationship between color parameter (RGB value) of BTB-loaded hydrogel and pH is shown in Fig. 3b–e. The biggest slope of linear equations was observed in Fig. 3d which originated from 0.04 % BTB-loaded hydrogel, indicating the most obvious color changes compared with other BTB-loaded hydrogels (Liu et al., 2022). BTB concentrations over 0.05 % were not tested because the coagulability of hydrogel became worse. Therefore, 0.04 % BTB was opted as the experimental concentration.

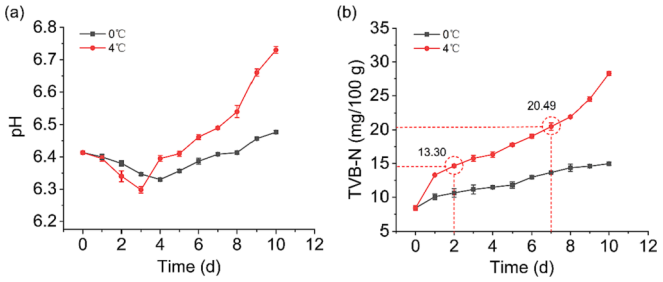

Fig. 4. (a) pH change of salmon during storage at 0 °C and 4 °C for 10 days. (b) TVB-N value of salmon stored at 0 °C and 4 °C for 10 days.

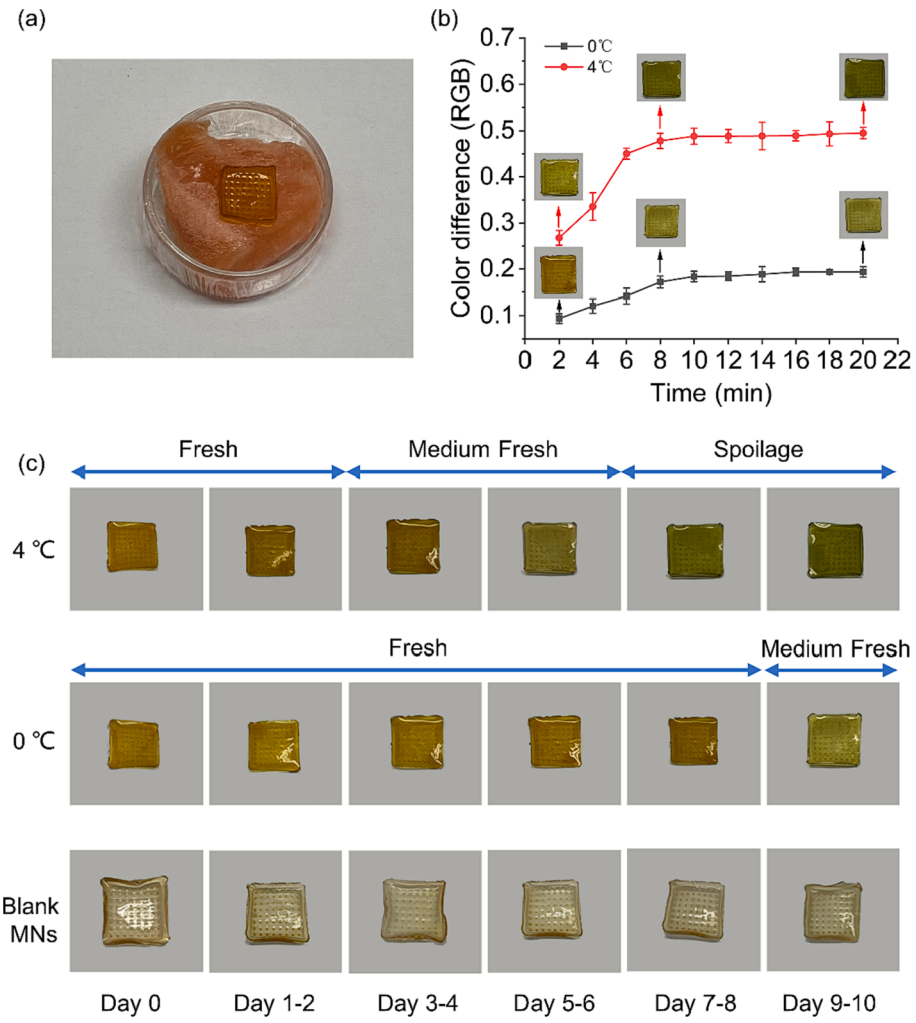

Fig. 5. (a) Photo of BTB/SilMA@MN patch as colorimetric sensor for salmon sampling. (b) Color response of BTB/SilMA@MN patch for salmons stored at 0 °C and 4 °C on day 10. (c) Color change of MN patches used to monitor the freshness of the salmon during storage.

3.5. Application of BTB/SilMA@MN patch for the detection of salmon spoilage

The color changes originating from BTB chromogenic dye of the BTB/SilMA@MN patch were caused by pH variation of salmon tissues due to TVB-N production. Thus, changes of pH, TVB-N, and some other properties were first discussed.

3.5.1. pH, TVB-N, TVC and other chemical and physical changes

Fig. 4a shows the pH change of salmon samples with time during storage. The initial pH of the salmon was 6.41 on day 0. After storage at 4 °C for 3 days, pH value reduced to 6.29 because glycolysis produced lactic acid accumulation. The pH increased to 6.46 and 6.73 after storage for 6 and 10 days, respectively, as a result of the production of ammonia and amines from protein decomposition (Moon, Kim, Xu, Na, Giaccia, & Lee, 2020). For the salmons stored at 0 °C, the pH decreased to the lowest 6.35 at day 4 and exceeded its initial pH value on day 9. Then, the final pH increased to 6.49 after 10 days storage. This trend in pH change of salmon is consistent with the results obtained by Ding et al (Ding, Li, & Li, 2014). Therefore, it is not accurate to use pH value for the detection of the salmon spoilage due to both pH decrease and increase could happen in storage. Thus, TVB-N and TVC were further detected.

TVB-N is the summation of ammonia, dimethylamine, trimethylamine and other basic nitrogenous substances produced after fish/meat spoilage (Prabhakar, Vatsa, Srivastav, & Pathak, 2020). TVB-N value is generally used as a quality indicator of fish/meat putrefaction (Fernández-Segovia, Fuentes, Aliño, Masot, Alcañiz, & Barat, 2012). According to Commission of the European Communities, a TVB-N value of $\leq$ 25 mg/100 g is considered as the acceptable limit for good-quality fish (European Commission, 1995). Specifically speaking, fish/meat with TVB-N value $\geq$ 20 mg/100 g is considered spoiled, 15–20 mg/100 g is medium fresh but cooking edible, and $\leq$ 15 mg/100 g represents fresh on the basis of previous report (Guo et al., 2020). Fig. 4b shows the change of TVB-N value in salmon during storage at 0 °C and 4 °C. The initial TVB-N value of salmon samples was 8.4 mg/100 g and the samples were identified as fresh. The TVB-N content gradually increased from the initial 8.4 mg/100 g to 20.5 mg/100 g on day 7 at 4 °C, indicating spoilage of salmon. However, the TVB-N content reached the maximum value of 15.0 mg/100 g at 0 °C after days storage, exhibiting the salmon samples were almost close to medium fresh.

TVC is a commonly used index to evaluate the degree of microbial contamination of aquatic products. According to the regulation of the International Committee on Microbiology for Food for raw salmon, the TVC of edible raw salmon should be $\leq$ 5 lg (CFU/g) (Ding, Li, & Li, 2014). Fig. S4 shows the TVC gradually increased from the initial 3.52 lg (CFU/g) to 5.26 lg (CFU/g) on the 7th day at 4 °C, indicating the salmon was inedible after a 7-day storage at 4 °C. However, the TVC reached the maximum value of 4.65 lg (CFU/g) on the 10th day after storage at 0 °C, exhibiting the salmon samples were still medium fresh after a 10-day storage at 0 °C. Meanwhile, the freshness classification of salmon

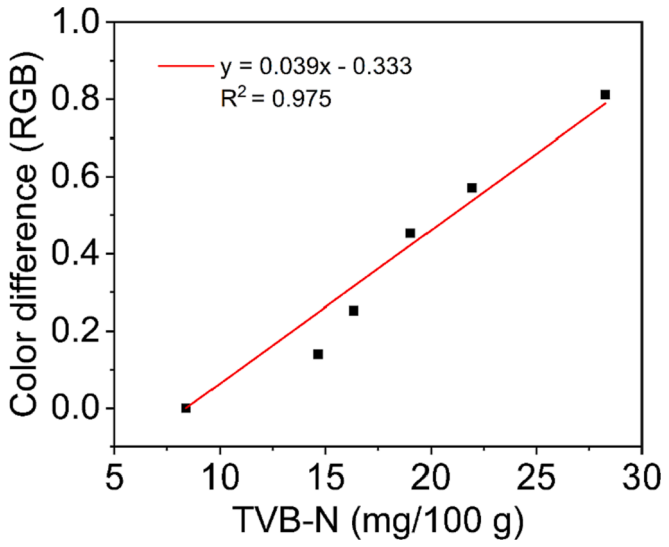

Fig. 6. Linear relationship between the RGB signal and TVB-N value of packaged salmons stored at 4 °C for 0, 2, 4, 6, 8, 10 days.

evaluated by TVC was consistent with the results of TVB-N.

The texture and histamine content of salmon stored at 0 and 4 °C for 10 days were also tested to evaluate the freshness of salmon (Feng, Zhang, Liu, Liu, & Zhang, 2020). The hardness, elasticity, chewiness and resilience of salmon all declined with the increase of storage time (Fig. S5). The histamine was 41.9 mg/kg of salmon stored at 4 °C on day 6, and increased to 54.2 mg/kg on day 7 (Fig S6), exceeding the limit value of histamine content (50 mg/kg) set by FDA (Surowka, Rzepka, Ozogul, Ozogul, Surowka, & Ligaszewski, 2021). These results are in good agreement with the above TVB-N values for distinguishing whether the fish spoiled.

3.5.2. Color change of BTB/SilMA@MN patch

BTB/SilMA@MN patch was inserted into salmon to indicate freshness/corruption using color displaying without destruction of packaging film (Fig. 5a). To test the color response of BTB/SilMA@MN patch for the detection of salmon spoilage in a rapid time, the patches were pasted on salmons stored at 0 °C and 4 °C on day 10 and color changes were recorded every 2 min. As shown in Fig. 5b. the RGB signal of color pictures obviously increased in the first 6 min and stabilized in the range of 8–20 min both for salmons stored at 0 °C and 4 °C, showing the MN patches could completely extract the liquid from the salmon sample at 8 min. When the MN patches were inserted on salmon, color changes indicating freshness/spoilage of samples could be realized quickly. The color of MN patch pasted on the salmon stored at 4 °C was initially yellow, indicating salmon fresh (Fig. 5c). Then, the color became deep yellow at day 3–4 and yellowish green at day 5–6. This stage was considered medium fresh. Finally, the color became green on day 7 and the green color sustained to the 10th day, representing spoiled and inedible fish. In addition, the color of MN patches on salmon stored at 0 °C on day 0–8 remained yellow and gradually changed to light green on day 9–10, stating the salmon were fresh for up to 8 days stored at 0 °C. The results show that the BTB/SilMA@MN patch could be used as a convenient colorimetric sensor for indicating salmon spoilage.

3.5.3. Correlation between color difference of BTB/SilMA@MN patch and TVB-N value

Fig. 6 shows the correlation between the RGB values calculated from color pictures of BTB/SilMA@MN patches and TVB-N value of salmon samples along with linear dependence model and the correlation coefficient (R^2). It is evident that a strong and positive correlation between the RGB values of the MN patch and the TVB-N values in salmon stored for 10 days. The results proved the colorimetric sensing ability of BTB/SilMA@MN patch for pH change originating from the increase of TVB-N. In other words, BTB/SilMA@MN patch can be a colorimetric indicator for indirect detection of TVB-N and the spoilage of packaged salmon.

4. Conclusion

In conclusion, we have developed colorimetric BTB/SilMA@MN patch using BTB as chromogenic dye and SilMA as hydrogel matrix for the detection of packaged salmon spoilage. The developed BTB/SilMA@MN patch exhibits strong mechanical strength and water absorption in the needles, allows easy penetrating food cling film and transporting inner food fluids to the backing layer in 8 min. The color change of BTB/SilMA@MN patch depends on the pH variation resulting from TVB-N increase in salmon during storage. Three stages (fresh - medium fresh - spoilage) of salmon freshness can be clearly distinguished from distinct color changes of the developed BTB/SilMA@MN patch. The developed BTB/SilMA@MN patch allows rapid detection of spoilage of packaged salmon with a mobile phone as detector in a nondestructive way, and shows great potential in food safety application.

CRediT authorship contribution statement

Jiang-Yue Wang: Methodology, Writing – original draft. **Li-Jian Chen:** Conceptualization, Writing – review & editing, Funding acquisition, Supervision. **Xu Zhao:** Methodology, Writing – review & editing. **Xiu-Ping Yan:** Project administration, Supervision, Conceptualization, Writing – review & editing, Funding acquisition.

Declaration of Competing Interest

The authors declare that they have no known competing financial interests or personal relationships that could have appeared to influence the work reported in this paper.

Data availability

Data will be made available on request.

Acknowledgements

The authors appreciate the financial support from the National Natural Science Foundation of China (No. 21934002), the Fundamental Research Funds for the Central Universities (No. JUSRP121005) and Collaborative Innovation Center of Food Safety and Quality Control in Jiangsu Province.

Appendix A. Supplementary data

Supplementary data to this article can be found online at https://doi.org/10.1016/j.foodchem.2022.135039.

References

Alamdari, N. G., Forghani, S., Salmasi, S., Almasi, H., Moradi, M., & Molaei, R. (2022). Ixiolirion tataricum anthocyanins-loaded biocellulose label: Characterization and application for food freshness monitoring. *International Journal of Biological Macromolecules, 200*, 87–98. https://doi.org/10.1016/j.ijbiomac.2021.12.188

Amagliani, G., Brandi, G., & Schiavano, G. F. (2012). Incidence and role of Salmonella in seafood safety. *Food Research International, 45*(2), 780–788. https://doi.org/10.1016/j.foodres.2011.06.022

Bae, S. B., Kim, M. H., & Park, W. H. (2020). Electrospinning and dual cross-linking of water-soluble silk fibroin modified with glycidyl methacrylate. *Polymer Degradation and Stability, 179*, Article 109304. https://doi.org/10.1016/j.polymdegradstab.2020.109304

Barroso, I. A., Man, K., Villapun, V. M., Cox, S. C., & Ghag, A. K. (2021). Methacrylated silk fibroin hydrogels: pH as a tool to control functionality. *ACS Biomaterials Science & Engineering, 7*(10), 4779–4791. https://doi.org/10.1021/acsbiomaterials.1c00791

Cao, L., Sun, G., Zhang, C., Liu, W., Li, J., & Wang, L. (2019). An intelligent film based on cassia gum containing bromothymol blue-anchored cellulose fibers for real-time detection of meat freshness. *Journal of Agricultural and Food Chemistry, 67*(7), 2066–2074. https://doi.org/10.1021/acs.jafc.8b06493

Chang, J., Li, H., Hou, T., Duan, W., & Li, F. (2018). Paper-based fluorescent sensor via aggregation induced emission fluorogen for facile and sensitive visual detection of hydrogen peroxide and glucose. *Biosensors and Bioelectronics, 104*, 152–157. https://doi.org/10.1016/j.bios.2018.01.007

Chen, H. Z., Zhang, M., Bhandari, B., & Guo, Z. (2018). Applicability of a colorimetric indicator label for monitoring freshness of fresh-cut green bell pepper. *Postharvest Biology and Technology, 140*, 85–92. https://doi.org/10.1016/j.postharvbio.2018.02.011

Cheng, J. H., & Sun, D. W. (2015). Rapid and non-invasive detection of fish microbial spoilage by visible and near infrared hyperspectral imaging and multivariate analysis. *LWT-Food Science and Technology, 62*(2), 1060–1068. https://doi.org/10.1016/j.lwt.2015.01.021

Cheng, K., Tao, X., Qi, Z., Yin, Z., Kundu, S. C., & Lu, S. (2021). Highly absorbent silk fibroin protein xerogel. *ACS Biomaterials Science & Engineering, 7*(8), 3594–3607. https://doi.org/10.1021/acsbiomaterials.1c00467

Ding, T., Li, T., & Li, J. (2014). Comprehensive evaluation on freshness of salmon slices at 0 °C storage. *Journal of Chinese Institute of Food Science and Technology, 14*(11), 252–259. https://d.wanfangdata.com.cn/periodical/zgspxb201411036.

Dixon, R. V., Skaria, E., Lau, W. M., Manning, P., Birch-Machin, M. A., Moghimi, S. M., & Ng, K. W. (2021). Microneedle-based devices for point-of-care infectious disease diagnostics. *Acta Pharmaceutica Sinica B, 11*(8), 2344–2361. https://doi.org/10.1016/j.apsb.2021.02.010

Commission, E. (1995). Commission decision of 8 March 1995 fixing the total volatile basic nitrogen (TVB-N) limit values for certain categories offishery products and specifying the analysis methods to be used. *Official Journal of the European Communities, 097*, 0084e0087.

Ezati, P., Priyadarshi, R., Bang, Y. J., & Rhim, J. W. (2021). CMC and CNF-based intelligent pH-responsive color indicator films integrated with shikonin to monitor fish freshness. *Food Control, 126*, Article 108046. https://doi.org/10.1016/j.foodcont.2021.108046

Fan, X., Lin, X., Wu, C., Zhang, N., Cheng, Q., Qi, H., … Dong, X. (2021). Estimating freshness of ice storage rainbow trout using bioelectrical impedance analysis. *Food Science & Nutrition, 9*(1), 154–163. https://doi.org/10.1002/fsn3.1974

Feng, H., Zhang, M., Liu, P., Liu, Y., & Zhang, X. (2020). Evaluation of IoT-enabled monitoring and electronic nose spoilage detection for salmon freshness during cold storage. *Foods, 9*(11), 1579. https://doi.org/10.3390/foods9111579

Fernández-Segovia, I., Fuentes, A., Aliño, M., Masot, R., Alcañiz, M., & Barat, J. M. (2012). Detection of frozen-thawed salmon (Salmo salar) by a rapid low-cost method. *Journal of Food Engineering, 113*(2), 210–216. https://doi.org/10.1016/j.jfoodeng.2012.06.003

Guo, L., Wang, T., Wu, Z., Wang, J., Wang, M., Cui, Z., … Chen, X. (2020). Portable food freshness prediction platform based on colorimetric barcode combinatorics and deep convolutional neural networks. *Advanced Materials, 32*(45), e2004805.

Kim, D., Lee, S., Lee, K., Baek, S., & Seo, J. (2017). Development of a pH indicator composed of high moisture-absorbing materials for real-time monitoring of chicken breast freshness. *Food Science and Biotechnology, 26*(1), 37–42. https://doi.org/10.1007/s10068-017-0005-6

Kim, S. H., Yeon, Y. K., Lee, J. M., Chao, J. R., Lee, Y. J., Seo, Y. B., … Park, C. H. (2018). Precisely printable and biocompatible silk fibroin bioink for digital light processing 3D printing. *Nature Communications, 9*(1), 2350. https://doi.org/10.1038/s41467-018-03759-y

Lee, K., Baek, S., Kim, D., & Seo, J. (2019). A freshness indicator for monitoring chicken-breast spoilage using a Tyvek® sheet and RGB color analysis. *Food Packaging and Shelf Life, 19*, 40–46. https://doi.org/10.1016/j.fpsl.2018.11.016

Li, H., Feng, J., Wang, Y., Liu, G., Chen, X., & Fu, L. (2021). Instant and multiple dna extraction method by microneedle patch for rapid and on-site detection of food allergen-encoding genes. *Journal of Agricultural and Food Chemistry, 69*(24), 6879–6887. https://doi.org/10.1021/acs.jafc.1c01077

Li, H., Lin, H., Wang, X., Lv, W., & Li, F. (2019). Dopamine-based paper analytical device for truly equipment-free and naked-eye biosensing based on the target-initiated catalyzed oxidation. *ACS Applied Materials & Interfaces, 11*(40), 36469–36475. https://doi.org/10.1021/acsami.9b14859

Li, H., Lin, H., Lv, W., Gai, P., & Li, F. (2020). Equipment-free and visual detection of multiple biomarkers via an aggregation induced emission luminogen-based paper biosensor. *Biosensors and Bioelectronics, 165*, Article 112336. https://doi.org/10.1016/j.bios.2020.112336

Liu, X., Chen, K., Wang, J., Wang, Y., Tang, Y., Gao, X., … Li, J. (2019). An on-package colorimetric sensing label based on a sol-gel matrix for fish freshness monitoring. *Food Chemistry, 307*, Article 125580. https://doi.org/10.1016/j.foodchem.2019.125580

Liu, L., Zhang, J., Zou, X., Arslan, M., Shi, J., Zhai, X., … Li, Y. (2022). A high-stable and sensitive colorimetric nanofiber sensor based on PCL incorporating anthocyanins for shrimp freshness. *Food Chemistry, 377*, Article 131909. https://doi.org/10.1016/j.foodchem.2021.131909

Moon, E. J., Kim, Y., Xu, Y., Na, Y., Giaccia, A. J., & Lee, J. H. (2020). Evaluation of salmon, tuna, and beef freshness using a portable spectrometer. *Sensors, 20*(15), 4299. https://doi.org/10.3390/s20154299

Park, T. S., Baynes, C., Cho, S. I., & Yoon, J. Y. (2014). Paper microfluidics for red wine tasting. *RSC Advances, 4*(46), 24356–24362. https://doi.org/10.1039/c4ra01471e

Prabhakar, P. K., Vatsa, S., Srivastav, P. P., & Pathak, S. S. (2020). A comprehensive review on freshness of fish and assessment: Analytical methods and recent innovations. *Food Research International, 133*, Article 109157. https://doi.org/10.1016/j.foodres.2020.109157

Rad, Z. F., Prewett, P. D., & Davies, G. J. (2021). An overview of microneedle applications, materials, and fabrication methods. *Beilstein Journal of Nanotechnology, 12*, 1034–1046. https://doi.org/10.3762/bjnano.12.77

Sun, Y., Liu, J., Wang, H., Li, S., Pan, X., Xu, B., … Liu, H. (2021). NIR laser-triggered microneedle-based liquid bandaid for wound care. *Advanced Functional Materials, 31*(29), 2100218. https://doi.org/10.1002/adfm.202100218

Surowka, K., Rzepka, M., Ozogul, F., Ozogul, Y., Surowka, B., & Ligaszewski, M. (2021). Nucleotide degradation, biogenic amine level and microbial contamination as quality indicators of cold-stored rainbow trout (*Oncorhynchus mykiss*) gravad. *Food Chemistry, 346*, Article 128904. https://doi.org/10.1016/j.foodchem.2020.128904

Sutthasupa, S., Padungkit, C., & Suriyong, S. (2021). Colorimetric ammonia (NH_3) sensor based on an alginate-methylcellulose blend hydrogel and the potential opportunity for the development of a minced pork spoilage indicator. *Food Chemistry, 362*, Article 130151. https://doi.org/10.1016/j.foodchem.2021.130151

Wu, D., Zhang, M., Chen, H., & Bhandari, B. (2021). Freshness monitoring technology of fish products in intelligent packaging. *Critical Reviews in Food Science and Nutrition, 61*(8), 1279–1292. https://doi.org/10.1080/10408398.2020.1757615

Yan, Q., Wang, W., Weng, J., Zhang, Z., Yin, L., Yang, Q., … Yang, G. (2020). Dissolving microneedles for transdermal delivery of huperzine A for the treatment of Alzheimer's disease. *Drug Delivery, 27*(1), 1147–1155. https://doi.org/10.1080/10717544.2020.1797240

Yang, J., Zhang, H., Hu, T., Xu, C., Jiang, L., Zhang, Y. S., & Xie, M. (2021). Recent advances of microneedles used towards stimuli-responsive drug delivery, disease theranostics, and bioinspired applications. *Chemical Engineering Journal, 426*, Article 130561. https://doi.org/10.1016/j.cej.2021.130561

Zhao, Y., Zhu, Z. S., Guan, J., & Wu, S. J. (2021). Processing, mechanical properties and bio-applications of silk fibroin-based high-strength hydrogels. *Acta Biomaterialia, 125*, 57–71. https://doi.org/10.1016/j.actbio.2021.02.018

Zhu, Z., Gao, H., Gao, T., & Sun, D.-W. (2018). Quality comparison of grass carp and salmon fillets packaged in modified atmosphere with different composite films. *Journal of Food Process Engineering, 41*(5), e12803.